JOURNAL OF DEGRADED AND MINING LANDS MANAGEMENT
Volume 11, Number 3 (April 2024):5623-5634, doi:10.15243/jdmlm.2024.113.5623
ISSN: 2339-076X (p); 2502-2458 (e), www.jdmlm.ub.ac.id

Research Article

Enhancing the estimation accuracy of above-ground carbon storage in *Eucalyptus urophylla* plantation on Timor Island, Indonesia, through higher spatial-resolution satellite imagery

Ronggo Sadono*, Emma Soraya

Department of Forest Management, Faculty of Forestry, Universitas Gadjah Mada, Jl. Agro No. 1 Bulaksumur, Sleman, Daerah Istimewa Yogyakarta 55281, Indonesia

*corresponding author: rsadono@ugm.ac.id

Article history:
Received 10 October 2023
Revised 10 January 2024
Accepted 27 January 2024

Keywords:
detailed object detection
Eucalyptus tree density
Pléiades imagery
remote sensing technology
very high spatial resolution

Abstract

Eucalyptus urophylla plantation is an important contributor to carbon storage in climate change mitigation, established due to a land rehabilitation program in the semi-arid ecosystem in Timor Island. To ensure an accurate estimate of the above-ground carbon storage of these plantations, it is important to continuously combine ground measurement with remote sensing technology. Therefore, this study aimed to compare the above-ground carbon storage estimation of two very high spatial resolution images, namely Pleiades-1B 2021 and Pléiades Neo 2022 with pixel sizes of 2 x 2 m and 1.2 x 1.2 m, respectively. The normalized difference vegetation index was employed to identify the eucalyptus trees and classify the density into low, moderate, and high. The results showed that Pléiades Neo imagery provided superior eucalyptus tree identification to Pleiades-1B imagery and was more accurate in estimating above-ground carbon storage. However, there is a trade-off between increasing this accuracy and incurring a higher cost to achieve the highest spatial resolution image.

To cite this article: Sadono, R. and Soraya, E. 2024. Enhancing the estimation accuracy of above-ground carbon storage in *Eucalyptus urophylla* plantation on Timor Island, Indonesia, through higher spatial-resolution satellite imagery. Journal of Degraded and Mining Lands Management 11(3):5623-5634, doi:10.15243/jdmlm.2024.113.5623.

Introduction

The successful rehabilitation from degraded land into plantation forests in dryland ecosystems is significantly important in enhancing above-ground carbon (AGC) storage and improving the sequestration of atmospheric carbon dioxide. The AGC per ha of barren, grass, and shrublands is approximately 2.5, 4.0, and 30.0 Mg C, respectively (Tosiani, 2015). In contrast, the *Eucalyptus urophylla* S.T. Blake plantation in dryland ecosystems at Timor Island, East Nusa Tenggara, Indonesia, was reported to have a maximum AGC of 128.57 Mg C ha^{-1} (Sadono et al., 2020a). The area was degraded area and has been rehabilitated using *E. urophylla* as an endemic species since 20 years ago. The introduction of improved intensive management, including the establishment of a forest management unit and commercial orientation, has accelerated reforestation in this area (Sadono et al., 2020a). However, it was also reported that the total carbon storage of *E. urophylla* plantations differ significantly in East Nusa Tenggara across the management types, including production, protection, and conservation forests (Marimpan et al., 2022). Achieving precise mapping of forest carbon stocks, a necessity for monitoring, reporting, and verification (MRV) to support local scale carbon management projects or national reporting within the frame of United Nations for reducing emissions from deforestation and degradation (UN REDD+), which would provide financial incentives for emissions reductions in developing countries, remains a challenging technical task (see: Mitchell et al., 2017). Satellite remote sensing emerges as a practical tool for

overseeing both forest cover and estimates of carbon stocks. Conversely, field plots provide accurate localized assessments of forest carbon stocks. Yet, the inherent natural variation in forest carbon density may hinder the effectiveness of plot-based approaches when extrapolating carbon estimates across large geographical areas. To estimate the potential carbon storage on a landscape scale, the density of the *E. urophylla* tree should be considered, as the stand density is strongly correlated with total carbon storage per ha. Monitoring and evaluating changes in land cover and carbon storage over time is important for determining whether there is an improvement or degradation, as well as carbon gain and loss.

Conventionally, carbon storage was estimated using the ground sampling method, coupled with allometric models of tree species found in plot sampling. These allometric models were constructed from previously selected destructive tree samples. The sampling design for field measurement is systematic (Sadono et al., 2020a) or clustered by considering the stand density, with low, medium, and high densities (Marimpan et al., 2022) to obtain the carbon storage per ha. The application of these estimates to larger scales is facilitated by the integration of remote sensing imagery using the forest canopy density (FCD) method (Sadono et al., 2020b). Kusuma et al. (2022) used Landsat 8 OLI imagery to assess the carbon storage in the Sisimeni Sanam Forest Area with Special Purpose on Timor Island, Indonesia, from 2013 to 2021, with a modified FCD method. Moreover, the FCD method could be used to estimate tree density and carbon storage, as evidenced by the findings in agroforestry land in East Kalimantan (Hartoyo et al., 2019) and secondary peat swamp forest in Central Kalimantan, Indonesia (Sukarna et al., 2021).

The availability and affordability of Pléiades images have created the possibility of accurately estimating the carbon storage of the plant community. This very high spatial resolution showed a high accuracy in plant community identification for the halophilic group of *Asteriscus* and the endemic *Chasmophyte* group of the Habibas archipelago (Hamimeche et al., 2021). Costa and Lameira (2022) employed a normalized difference index (NDVI) to characterize vegetation structure in the municipality of Moju-PA and the city of Belém-PA using Pléiades images. Apart from detecting accurate land cover, the use of NDVI with Pléiades satellite imagery can also classify the density of the investigated tree area. According to the underlying theory, a higher NDVI corresponds to denser tree cover (Sadono et al., 2023a). In cases where high precision is necessary due to the value of the species being monitored, a higher spatial resolution satellite image becomes imperative. The Pléiades Neo image, which has a higher spatial resolution compared to the previous Pléiades image, emerges as a viable solution to meet the precision challenge. This study aimed to detect the changes in carbon storage of *E. urophylla* stands that were planted on degraded land on Timor Island in East Nusa Tenggara, Indonesia, using higher spatial resolution satellite imageries, specifically the Pléiades Neo 2022 image compared to Pléiades-1B 2021 image as a reference of investigation.

Materials and Methods

Eucalyptus urophylla plantation description

This study is an integral part of a larger investigation that was initiated in 2020, focusing on biomass and carbon storage estimation, as well as the potential of eucalyptus plantations as a renewable energy source. The area of interest is ca. 27 hectares of eucalyptus plantation located in South Central Timor Regency. The plantation was managed by the Timor Tengah Selatan Forest Management Unit and was intended for commercial plantation forest (Sadono et al., 2020a). The area has a geographic coordinate ranging from 9º50′0″ to 9º50′22″ S and 124º15′32″ to 124º15′55″ E, located in the Universal Transverse Mercator/WGS84-51S zone from 8912750 to 8912000 S and from 638000 to 638750 E. Administratively, the area is a part of three villages, consisting of Noinbila, Nonohonis, and Biloto, which were located in the north, east to the south, and in the west, respectively (Figure 1).

The *Eucalyptus urophylla* plantation exhibited a high variation in tree density per ha, with a 62.09% coefficient of variation. The average stand density was 182 trees ha^{-1}, with the minimum and maximum densities being 59 and 620 trees ha^{-1}, respectively. The high variation was also shown in basal area and volume per ha, which were 56.05 and 59.85%, respectively. However, diameter and height exhibited low variation, with coefficients of variation being 13.87 and 7.01%. Due to the low coefficient of variation in tree height, the canopy was divided into two strata, namely dominant and co-dominant layers. The great variation in tree densities also contributed to differences in carbon storage across all parts of the tree, ranging from 57.57 to 61.13%. Consequently, the total carbon storage per ha varied significantly, with a coefficient of variation being 60.54% (Table 1).

Materials

Pléiades-1B imagery acquired on 10/09/2021 and Pléiades Neo imagery obtained on 25/10/2022 were used as the basis for change detection in carbon storage. Both sets of imagery were georeferenced in the UTM/WGS84—51S coordinate system and were obtained from a satellite imagery provider (https://www.geo-circle.com/). Furthermore, Pléiades-1B and Pléiades Neo multispectral images exhibited spatial resolutions of 2 m and 1.2 m, respectively (Table 2). Both images were pre-processed with radiometric and geometric correction before being clipped to display in the study area. These prepared

images, ready for further analysis, were depicted at the top and bottom to allow for easy visual comparison (Figure 2).

Data analysis

The normalized difference vegetation index (NDVI) is employed to classify land cover class (Abdullah et al., 2019; Hashim et al., 2019; Arini et al., 2020; Aryal et al., 2022). The NDVI index has minimum and maximum values of -1 and +1 for non-vegetated and fully stocked vegetated areas, respectively. A higher NDVI index value indicates that there is more vegetation on the ground.

Based on previous investigations, *E. urophylla* trees were identified using Sentinel-2B satellite imagery and an NDVI threshold value of approximately 0.7 (Sadono et al., 2023a). The Pléiades satellite imagery showed that the *E. urophylla* tree had an NDVI value greater than 0.699 (Sadono et al., 2023b). Furthermore, non-eucalyptus tree areas were divided into non-forest with NDVI values less than 0.5, and open-forest ranging from 0.5 to 0.699.

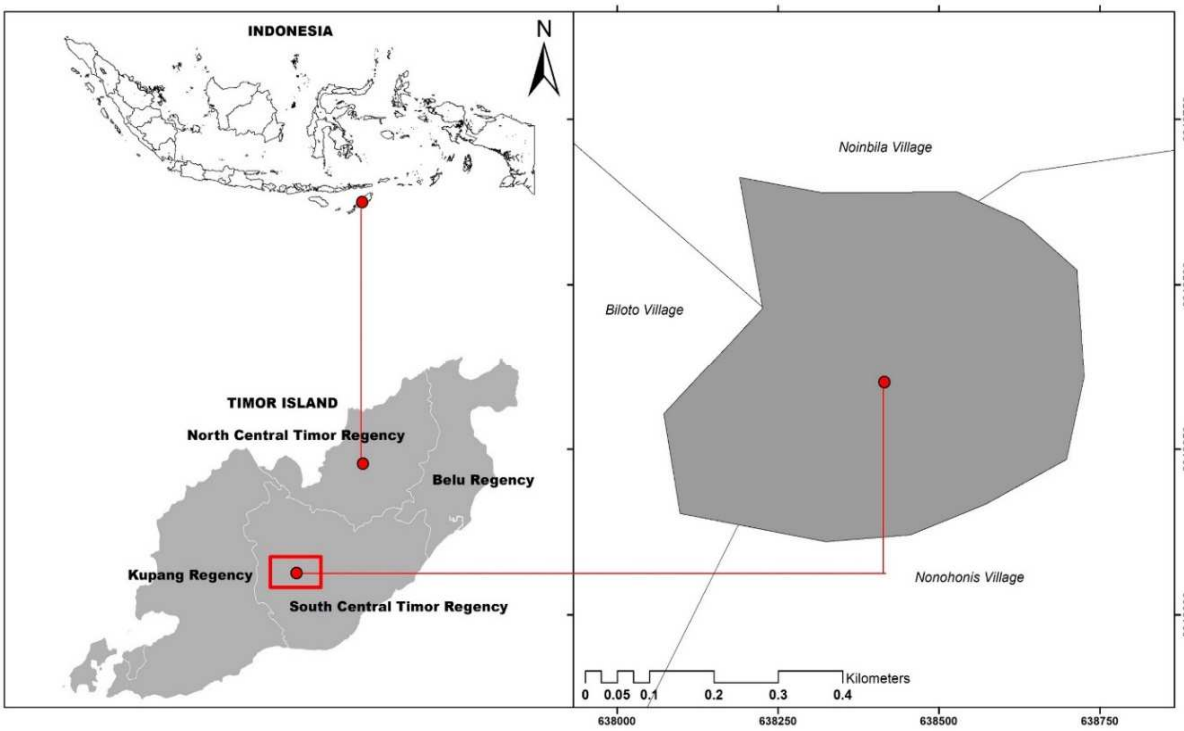

Figure 1. The study site of *Eucalyptus urophylla* S.T. Blake plantation part of Noinbila, Nonohonis, and Biloto Villages, South Central Timor Regency on Timor Island, Indonesia.

Table 1. The stand characteristics and carbon storage of *Eucalyptus urophylla* plantation based on previous field 36 plots sampling measurement (Sadono et al., 2020a).

Parameters	Minimum	Maximum	Mean	Standard deviation	Coefficient of variation (%)
Stand characteristics:					
Tree density (trees ha^{-1})	59	620	182	113	62.09
Diameter (cm)	23.70	43.31	33.01	4.68	13.87
Height (m)	24.77	33.44	29.39	2.06	7.01
Basal area (m^2 ha^{-1})	4.60	44.61	17.11	9.59	56.05
Volume (m^3 ha^{-1})	40.36	427.81	150.12	89.55	59.65
Carbon storage (Mg ha^{-1}):					
Root	1.98	23.71	8.23	4.95	60.15
Stem	7.95	99.59	33.65	20.57	61.13
Branch	1.96	22.62	8.02	4.76	59.35
Foliage	0.41	4.23	1.60	0.92	57.50
Total	12.48	152.28	52.25	31.63	60.54

Table 2. The satellite imagery characteristics: bands, wavelength, and spatial resolution of Pléiades-1B (Alcaras et al., 2022) and Pléiades Neo (Hestrio et al., 2021).

Satellite imagery	Bands	Wavelength (nm)	Spatial resolution (m)
Pléiades-1B	Blue	430-550	2.0
	Green	490-610	2.0
	Red	600-720	2.0
	Near infra-red (Nir)	750-950	2.0
	Panchromatic (Pan)	480-830	0.5
Pléiades Neo	Deep Blue	400-450	1.2
	Blue	430-520	1.2
	Green	530-590	1.2
	Red	620-690	1.2
	Red Edge	700-750	1.2
	Near infra-red (Nir)	770-880	1.2
	Panchromatic (Pan)	450-800	0.3

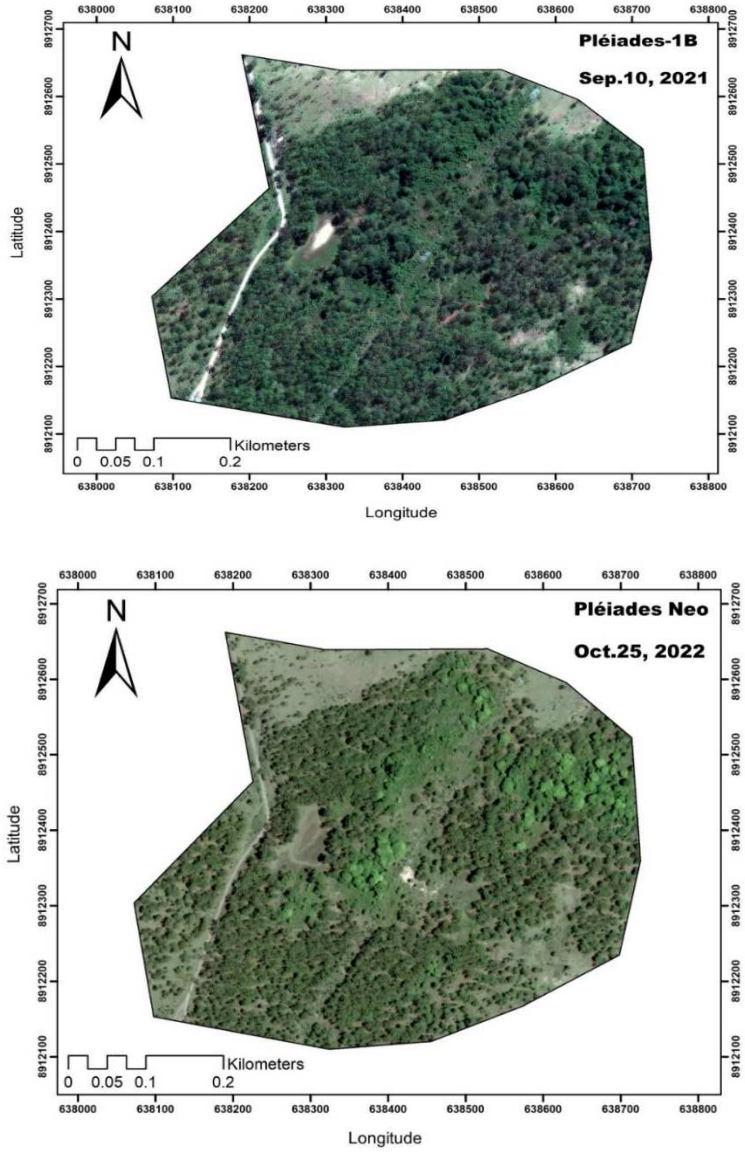

Figure 2. Satellite imagery covered the study area of ca. 27 ha and georeferred in the UTM/WGS84—51S zone coordinates: true color RGB composition of bands pre-processed with geometric and radiometric correction: Pléiades-1B acquired on September 10, 2021 (top, source: Sadono et al. 2023b), and Pléiades Neo acquired on October 25, 2022 (bottom).

The density of eucalyptus trees was classified into three levels based on the range of obtained NDVI values for *E. urophylla* plantation by Pleiades Neo 2022 as a reference, with the same interval representing low, moderate, and high tree density. These categories were transformed into three levels of stand density, including low, moderate, and high. According to Sadono et al. (2020a), the moderate density was equal to the average total carbon storage of 52.25 Mg C ha^{-1}, while the low density was obtained by subtracting the average density with a standard deviation. Meanwhile, the high density was calculated by adding the average density with a standard deviation.

Based on this assumption, the total carbon storage for low and high densities obtained were 20.62 and 83.88 Mg C ha^{-1}, respectively. The total carbon storage of the *E. urophylla* plantation in the study area was calculated by summing up the product of the assumed total carbon storage for each tree density and the corresponding calculated area.

Results and Discussion

The NDVI value was obtained based on the calculation of the near-infrared (NIR) and red band from the satellite imagery used (Viana et al., 2012; Hashim et al., 2015; Sadono et al., 2023b). Meanwhile, the NDVI digital map obtained from Pléiades Neo satellite imagery in 2022 showed more red color sparsely distributed over the study area compared to Pléiades-1B satellite imagery in 2021. The rapidly expanding area was shown in yellow, and the Pléiades Neo satellite imagery made the open forest more visible in 2022. As illustrated in Figure 3, Pléiades Neo satellite imagery from 2022 reduced green color, indicating that eucalyptus trees were more easily detected and distinguished from open forests.

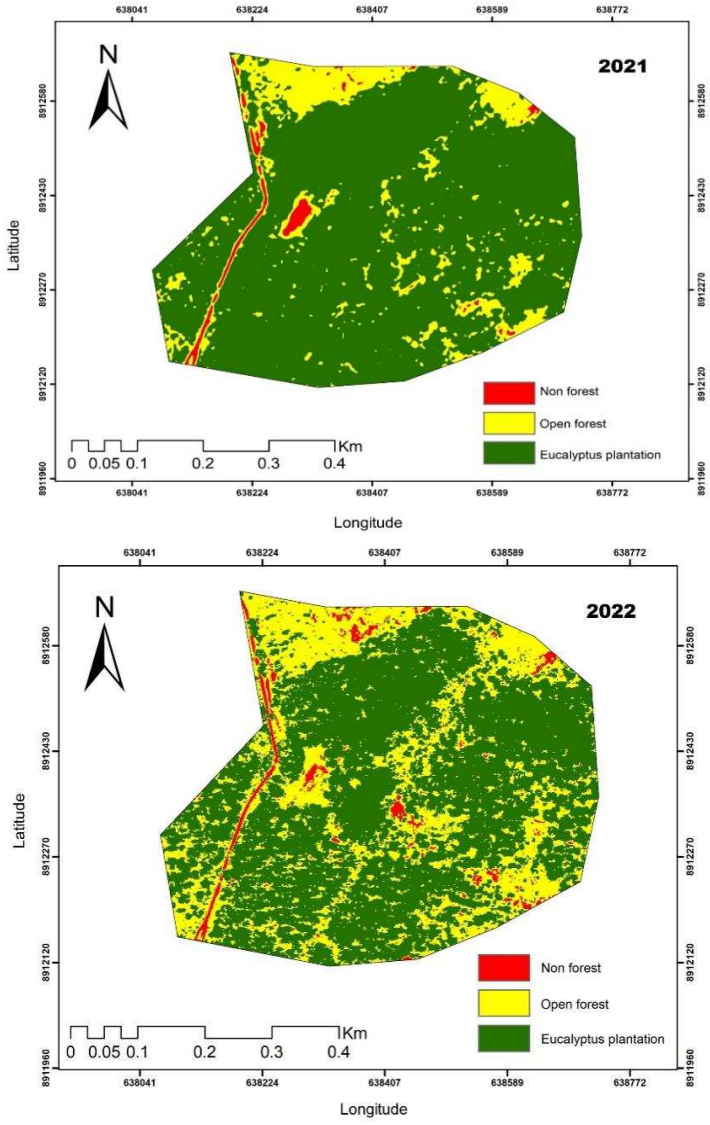

Figure 3. The NDVI map exhibits that eucalyptus trees are not completely covering the study area and that occupancy is visibly lower in 2022 (bottom: Pléiades Neo) than in 2021 (top: Pléiades-1B).

For Pléiades-1B satellite imagery in 2021, the calculated NDVI values ranged from -0.25 to 0.901, while Pleiades Neo 2022 satellite imagery yielded -0.008 to 0.917. According to the NDVI histogram, the frequency of NDVI values in 2021 was mostly around 0.8 in Pléiades-1B satellite imagery. However, the majority of NDVI values in Pleiades Neo 2022 satellite imagery had shifted closer to 0.85 (Figure 4).

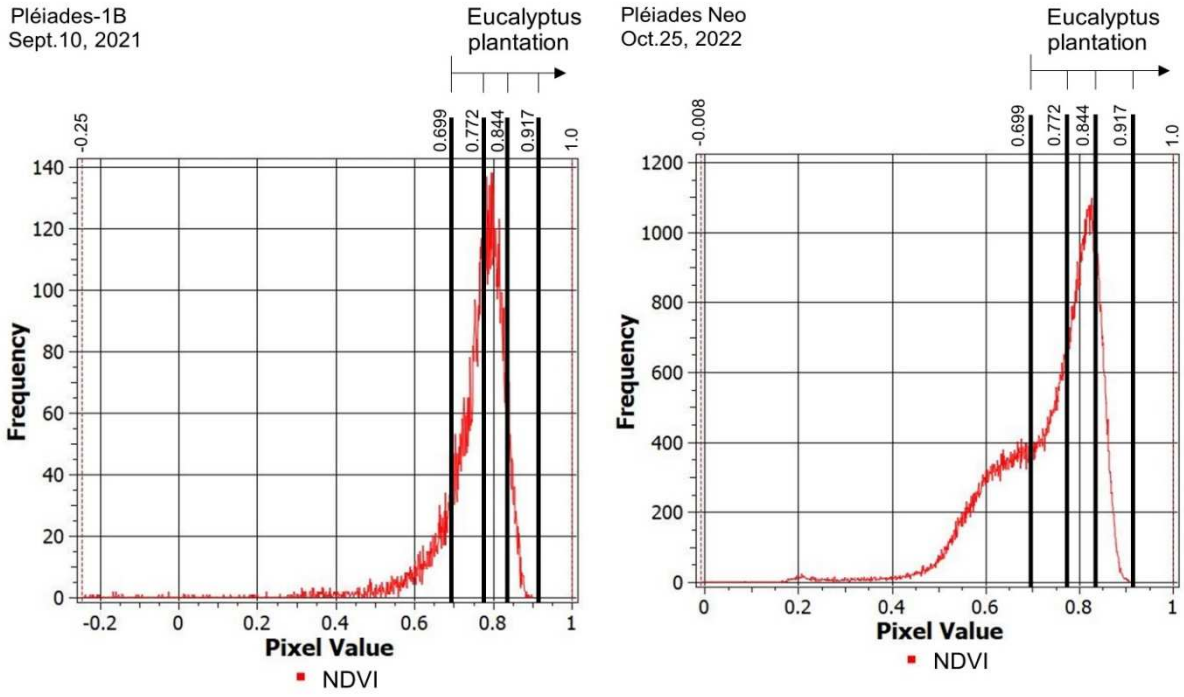

Figure 4. Histogram of NDVI values distribution with identified eucalyptus plantation, Pléiades-1B satellite imagery in 2021 (left), and Pléiades Neo satellite imagery in 2022 (right).

NDVI for land cover classification

Previous investigations had commonly employed NDVI to detect and classify vegetation communities and land use/land cover using a variety of satellite imageries with different levels of spatial resolution. The use of higher-resolution satellite imagery typically improved the accuracy of vegetation community and land use/land cover detection and classification. Sentinel-2 multispectral satellite imagery with a spatial resolution of 10 m outperformed Landsat 8 OLI multispectral satellite imagery with a spatial resolution of 30 m on land use/land cover mapping in Saqqez, Kurdistan Province, west Iran (Ghayour et al., 2021). Based on an investigation of land use/land cover in Kabul, the capital city of Afghanistan, the overall accuracy for Sentinel-2 and Landsat 8 OLI was 94.26% and 85.04%, while the Kappa coefficient was 91.7% and 78.3%, respectively (Ahady and Kaplan, 2022).

A previous study conducted in 2018, comparing various spatial resolutions of satellite imageries for detecting and classifying mangrove species communities showed that the accuracy level in descending order was Pléiades-1, Sentinel-2A, and Landsat 8 OLI satellite imageries, with a classification accuracy of 78.57%, 70.95%, and 68.57%, respectively (Wang et al., 2018). On land use/land cover mapping in Algerian island vegetation, Pléiades-1 multispectral satellite imagery with a spatial resolution of 2 m outperformed SPOT 6/7, which exhibited a resolution of 6 m. The overall accuracy for the Pléiades and SPOT 6/7 was >92% and >83, with the Kappa index of >0.90 and >0.80, respectively (Hamimeche et al., 2021). Pléiades satellite imagery has been employed in several investigations to detect and classify land use/land cover using NDVI (Hashim et al., 2019; Arini et al., 2020; Pu et al., 2018). The results showed that NDVI obtained from the Pléiades image was reliable for detecting and classifying land cover with a very high accuracy. However, the effective application of NDVI was dependent on the quality of multispectral data and the interpretation of NDVI values (Huang et al., 2021).

The NDVI threshold for classifying land cover was significantly influenced by the nature of the investigated object. Hashim et al. (2019) employed three vegetation classes in urban vegetation using Pléiades satellite imagery. This classification included non-vegetation, low vegetation, and high vegetation with NDVI thresholds of -1 to 0.199, 0.2 to 0.5, and 0.501 to 1.0, respectively. According to Larekeng et al.

(2022), the NDVI value range for shrubs was 0.5 to 0.6, low-density forests were 0.6 to 0.65, and medium-density forests were 0.65 to 0.7. Furthermore, Sadono et al. (2023a) classified the land cover of Mutis Timau Nature Reserve using Sentinel-2 satellite imagery with an NDVI threshold of 0.7 to differentiate eucalyptus plantations. An NDVI value equal to or above this threshold was identified and classified as a eucalyptus area. Detecting and classifying land cover in a eucalyptus plantation was relatively easier, particularly when using very high spatial resolution imagery, as there was only one investigated tree species on the ground. Sadono et al. (2023b) reported that the NDVI threshold for eucalyptus plantations was ≥0.7.

NDVI for densities classification and carbon storage estimation

The NDVI value had been widely adopted for classifying vegetation, stand, and tree densities in the field, with the underlying theory being that the higher the NDVI value, the denser the vegetation, stand, or trees in the field. However, the accuracy of classification with NDVI measurements was significantly impacted by biophysical characteristics of the canopy and growth environment, such as vegetation cover, biomass, plant, and soil moisture, as well as the effect of the measuring equipment, including satellite drift, calibration uncertainties, and atmospheric conditions factors (Duan et al., 2017). Samsuri et al. (2021) employed Sentinel 2A satellite imagery to classify mangrove tree density into four categories, namely low, moderate, high, and very high, which corresponded to the number of trees per ha. Wang et al. (2018) reported that NDVI was reliable for identifying trees and predicting stand density using QuickBird images. Recently, Han and Xu (2022) found that NDVI can effectively identify trees and correlate with stand density using high-resolution remote sensing imagery. In addition to using Sentinel 2B, Sadono et al. (2023a) classified eucalyptus vegetation into three densities based on NDVI interval in ascending values, namely low, moderate, and high densities. Sadono et al. (2023b) recently investigated the use of Pléiades 1 satellite imagery to classify a eucalyptus plantation into three densities, namely low, moderate, and high trees based on NDVI intervals in ascending values.

Regardless of the specific satellite imagery used, observation had shown that higher NDVI values were associated with greater carbon storage. The correlation values ranged from moderate to strong depending on the investigated area of interest. Marelign and Mekonen (2022) discovered a 0.86 correlation between NDVI and above-ground carbon storage in the Dirmaga Watershed in Ethiopia. In 2022, the correlation value obtained between NDVI and carbon storage in Tiru-Selam Forest, North-western Ethiopia, was 0.74 (Gashu and Marelign, 2022). Devkota et al. (2023) found a moderate correlation between NDVI and carbon storage at study sites in Nepal's Kanchanpur and Kailali districts to be 0.54 and 0.382, respectively. Furthermore, Shah and Sharma (2023) from the Indian Himalaya Region reported correlation coefficients of 0.74 and 0.67. Marimpan (2023) also showed that the correlation values between NDVI and carbon storage of eucalyptus vegetation in East Nusa Tenggara, Indonesia, were 0.88, 0.68, and 0.81, for production, protected, and conservation forest, respectively. In summary, NDVI exhibited a significant positive linear relationship with carbon storage, particularly in vegetated land.

According to the Pléiades-1B satellite imagery in 2021, the area composition classified based on NDVI value and identified as non-forest, open forest, and eucalyptus plantation was 0.42, 3.91, and 22.71 ha, respectively. This composition was significantly altered in 2022, with the addition of non-forest, the extension of open forest, and a significant decrease in eucalyptus plantations, resulting in areas of 0.27, 4.18, and -4.45 ha, respectively. As shown in Table 3, according to Pléiades Neo satellite imagery in 2022, the area composition was comprised of 0.69, 8.09, and 18.26 ha, representing non-forest, open forest, and eucalyptus plantation, respectively. With Pléiades-1B satellite imagery, the area for eucalyptus plantation in 2021 was 22.71 ha. This total area was divided into low, moderate, and high-density areas of 8.01, 12.87, and 1.83 ha, respectively. Meanwhile, the total area for eucalyptus plantation in 2022 was calculated using Pléiades Neo satellite imagery and was classified as low, moderate, and high density, with areas of 5.28, 10.42, and 2.55 ha, respectively. In 2022, low and moderate densities decreased by 2.73 and 2.44 ha, respectively, while high density increased by 0.72 ha (Table 3).

The shift in the composition of the identified eucalyptus plantations in 2022 was primarily derived from previously categorized as non-forest and open forest, accounting for less than one ha. In 2021, the majority of the eucalyptus plantations covered an area of 0.004, 0.750, and 17.51 ha, respectively. Meanwhile, in 2022, the remaining covering area of 22.71 ha was identified as eucalyptus plantations of 0.12, 5.08, and 17.51, respectively. More than 60% of all land cover remained consistent between 2021 and 2022, including 66.1, 73.4, and 77.1% for non-forest, open-forest, and eucalyptus plantations, respectively (Table 4).

The shift in the composition of eucalyptus plantation identification in 2022 was derived from less than a hectare of non-forest and open forest. This also included the majority of eucalyptus plantations in 2021, covering an area of 0.004, 0.750, and 17.51 ha, respectively. However, a cover area of 22.71 ha was classified as non-forest, open-forest, and *Eucalyptus plantation* with 0.12, 5.08, and 17.51 ha, respectively. As presented in Table 5, more than 60% of all land cover remained the same in 2021 and 2022, including

66.1, 73.4, and 77.1% for non-forest, open-forest, and *E. urophylla* plantations, respectively. The spatial distribution of eucalyptus plantation density showed that the high density in 2022 extended the area in the center from moderate density in 2021, regardless of growth or increment of open forest and eucalyptus plantation. Other areas of high density in 2021 tended to decrease into moderate and low densities in 2022, particularly in the north and east of the investigated area. In 2021, the shift of eucalyptus plantations with low and moderate density was predominantly identified in 2022 as open forest, with a small portion designated as non-forest, as illustrated in Table 6 and Figure 5.

Table 3. Estimated area distribution over land cover in 2021 and 2022, as well as the change in area between 2022 and 2021.

NDVI interval	Land cover	Estimated area 2021 (ha)[1]	Estimated area 2022 (ha)[2]	Change area (ha) 2022-2021
> -0.25 - 0.500	Non forest	0.42	0.69	0.27
> 0.500 - 0.699	Open forest	3.91	8.09	4.18
> 0.699 - 0.917	Eucalyptus plantation	22.71	18.26	-4.45
		27.04	27.04	
> 0.699 - 0.772	Low density	8.01	5.28	-2.73
> 0.772 - 0.844	Moderate density	12.87	10.43	-2.44
> 0.844 - 0.917	High density	1.83	2.55	0.72

Note: [1]Pléiades-1B satellite imagery and [2]Pléiades Neo satellite imagery.

Table 4. Shifts in the identification of eucalyptus plantations from 2021 to 2022 in ha and (%).

Year		2022			
	Land cover	Non forest	Open forest	Eucalyptus plantation	Total
2021	Non forest	0.28 (66.1%)	0.14	0.004	0.42
	Open forest	0.29	2.87 (73.4%)	0.750	3.91
	Eucalyptus plantation	0.12	5.08	17.510 (77.1%)	22.71
	Total	0.69	8.09	18.263	27.04

Table 5. Shifts in the identification of eucalyptus plantation area in ha and (%) over density in 2021 using Pléiades-1B satellite imagery and in 2022 using Pléiades Neo satellite imagery.

Year		2022			
	Eucalyptus plantation density	Low density	Moderate density	High density	Total
2021	Low density	2.14 (43.1%)	2.57	0.24	4.95
	Moderate density	2.87	7.13 (62.2%)	1.47	11.47
	High density	0.27	0.72	0.85 (46.2%)	1.83
	Total	5.28	10.43	2.55	18.26

Table 6. The shifting of land cover area distribution in ha from 2021 using Pléiades-1B satellite imagery to 2022 using Pléiades Neo satellite imagery.

Year	Land cover	2022					
		Non forest	Open forest	Eucalyptus plantation			Total
				Low density	Moderate density	High density	
2021	Non forest	0.28	0.14	0.00	0.00	0.00	0.42
	Open forest	0.29	2.87	0.39	0.34	0.02	3.91
	Eucalyptus plantation						
	Low density	0.09	3.19	2.14	2.13	0.46	8.01
	Moderate Density	0.03	1.85	2.64	7.13	1.22	12.87
	High density	0.00	0.04	0.11	0.82	0.85	1.83
	Total	0.69	8.09	5.28	10.43	2.55	27.04

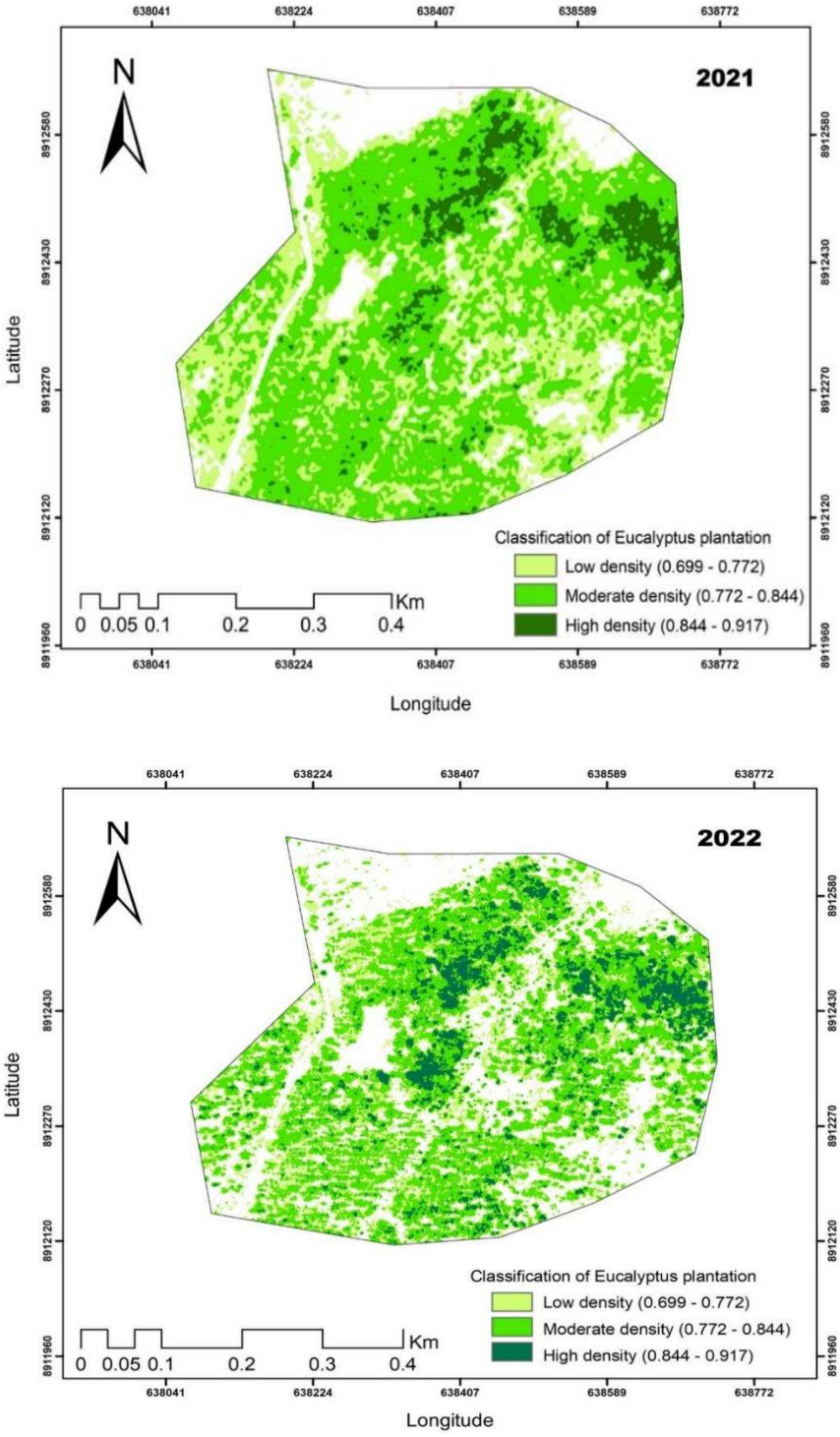

Figure 5. The spatial distribution of over-density eucalyptus plants in 2021 as depicted by Pléiades-1B satellite imagery (top) and in 2022 as depicted by Pléiades Neo satellite imagery (bottom).

The use of Pléiades-1B satellite imagery and a 22.71 ha eucalyptus plantation showed an estimated carbon of 990.76 Mg C in 2021, which was divided into low, moderate, and high densities of 165.11, 672.22, and 153.43 Mg C, respectively. The estimated carbon area of 18.26 ha in 2022, using Pléiades Neo satellite imagery, was 867.61 Mg C, with 108.98, 544.73, and 213.90 MgC for low, moderate, and high densities, respectively. This indicated that carbon estimates at low and moderate densities were reduced by 56.13 and 127.48 Mg C. However, there was an additional carbon estimate at a high density of 60.47 Mg C and a 123.14 Mg C difference in estimated carbon between 2021 and 2022 (Table 7).

Table 7. Estimated carbon storage over eucalyptus plantation density, as well as the change in carbon storage between 2022 using Pléiades Neo satellite imagery and 2021 using Pléiades-1B satellite imagery.

Density of Eucalyptus plantation	Estimated carbon storage in 2021 (Mg C)	Estimated carbon storage in 2022 (Mg C)	Change in carbon storage between 2022-2021 (Mg C)
Low	165.11	108.98	-56.13
Moderate	672.22	544.73	-127.48
High	153.43	213.90	60.47
Total	990.76	867.61	-123.14

Remote sensing technology is constantly improving, providing very high spatial resolution images, such as Pléiades-1B and Pléiades Neo, with resolutions of 2 m and 1.2 m, respectively. Pleades-1B imagery, with a pixel size of 2 x 2 m, can cover a single *E. urophylla* tree with a tree crown diameter of 2 m (Jaelani and Putri, 2019). Meanwhile, Pléiades Neo imagery with a pixel size of 1.2 x 1.2 m can cover an individual tree with a crown diameter of 1.2 m (Hestrio et al., 2021). The Pléiades Neo imagery can also separate eucalyptus trees in greater detail compared to the Pleiades-1B imagery. This phenomenon indicates that Pléiades Neo imagery can provide eucalyptus tree identification superior to Pleiades-1B imagery.

Based on its superiority in eucalyptus tree identification, the Pléiades Neo imagery is also more effective in providing corresponding stand density. Moreover, the use of GIS software such as QGIS allows natural resource managers to observe spatial patterns of land cover in geographic areas (Flenniken et al., 2020). This density information is precisely identified as a finer vegetation index. Above-ground carbon storage based on the eucalyptus stand density class can also be estimated more accurately by classifying NDVI obtained from finer indexes (Hestrio et al., 2020).

Conclusion

In conclusion, this study showed the importance of continuous and accurate estimation of carbon storage in plantation forests in the context of climate change mitigation. For large areas of interest, the NDVI class and estimated carbon storage in each class that upscaled using Pléiades Neo imagery produced a more accurate result compared to Pleiades-1B imagery. However, the superior accuracy of Pléiades Neo in estimating above-ground biomass storage should be offset by the cost of imagery provision. The increased accuracy estimation achieved from Pleiades-1B to Pléiades Neo needs to be tripled, resulting in a significantly high cost.

Acknowledgments

The author is grateful to Adhe Viana Yulida Putri for providing unwavering support and assistance with image processing.

References

Abad-Segura, E., González-Zamar, M.D., Vázquez-Cano, E. and López-Meneses, E. 2020. Remote sensing applied in forest management to optimize ecosystem services: advances in research. *Forests* 11(9):969, doi:10.3390/f11090969.

Abdullah, A.Y.M., Masrur, A., Adnan, M.S.G., Baky, M.A.Al., Hassan, Q.K. and Dewan, A. 2019. Spatio-temporal patterns of land use/land cover change in the heterogeneous coastal region of Bangladesh between 1990 and 2017. *Remote Sensing* 11:790, doi:10.3390/rs11070790.

Ahady, A.B. and Kaplan, G. 2022. Classification comparison of Landsat-8 and Sentinel-2 data in Google Earth Engine, study case of the city of Kabul. *International Journal of Engineering and Geosciences* 7(1):24- 31, doi:10.26833/ijeg.860077.

Alemu, B. 2014. The role of forest and soil carbon sequestrations on climate change mitigation. *Research Journal of Agriculture and Environmental Management* 3(10):492-505.

Arini, D., Guvil, Q. and Wahidah, N. 2020. Land cover identification using Pleiades satellite imagery by comparison of NDVI and BI method in Jatinangor, West Java. *IOP Conference Series: Earth and Environmental Science* 500:012007, doi:10.1088/1755-1315/500/1/012007.

Aryal, J., Sitaula, C. and Aryal, S. 2022. NDVI Threshold-based urban green space mapping from Sentinel-2A at the local governmental area (LGA) level of Victoria, Australia. *Land* 11:351, doi:10.3390/land11030351.

Barbierato, E., Bernetti, I., Capecchi, I. and Saragosa, C. 2020. Integrating remote sensing and street view images to quantify urban forest ecosystem services. *Remote Sensing* 12(2):329, doi:10.3390/rs12020329.

Chen, M., Qiu, X., Zeng, W. and Peng, D. 2022. Combining sample plot stratification and machine learning algorithms to improve forest above-ground carbon density estimation in Northeast China Using Airborne LiDAR Data. *Remote Sensing* 14:1477, doi:10.3390/rs14061477.

Costa, A.S. and Lameira, O.A. 2022. The use of NDVI derived from Pléiades images in the analysis of the vegetation structure in two forest fragments. *Research, Society and Development* [S. l.] 11(1):e54711124170, doi:10.33448/rsd-v11i1.24170.

Devkota, S., Mandal, R.A. and Khadka, A. 2023. Assessing the correlation between above-ground carbon stock, NDVI and tree species diversity (A study of Kailali and Kanchanpur District). *International Journal of World Policy and Development Studies* 9(1):11- 18, doi:10.32861/ijwpds.91.11.18.

Duan, T., Chapman, S.C., Guo, Y. and Zheng, B. 2017. Dynamic monitoring of NDVI in wheat agronomy and breeding trials using an unmanned aerial vehicle. *Field Crops Research* 210:71-80, doi:10.1016/j.fcr.2017.05.025.

Ekoungoulou, R., Liu, X., Ifo, S.A., Loumeto, J.J. and Folega, F. 2014. Carbon stock estimation in secondary forest and gallery forest of Congo using allometric equations. *International Journal of Scientific & Technology Research* 3(3):465-474.

Flenniken, J.M., Stuglik, S. and Iannone, B.V. 2020. Quantum GIS (QGIS): An introduction to a free alternative to more costly GIS platforms: FOR359/FR428, 2/2020. *EDIS* 2020(2):7-7.

Gashu, E.G. and Marelign, M.A. 2022. Estimation of carbon stock using ground inventory and remote sensing imagery in the case of Tiru-Selam Forest, North-western Ethiopia. *Computational Ecology and Software* 12(3):141- 153.

Ghayour, L., Neshat, A., Paryani, S., Shahabi, H., Shirzadi, A., Chen, W., Al-Ansari, N., Geertsema, M., Amiri, M.P., Gholamnia, M., Dou, J. and Ahmad, A. 2021. Performance evaluation of Sentinel-2 and Landsat 8 OLI data for land cover/use classification using a comparison between machine learning algorithms. *Remote Sensing* 13:1349, doi:10.3390/rs13071349.

Hamimeche, M., Niculescu, S., Billey, A. and Moulaï, R. 2021. Identification and mapping of Algerian island vegetation using high-resolution images (Pléiades and SPOT 6/7) and random forest modeling. *Environmental Monitoring and Assessment* 193:617, doi:10.1007/s10661-021-09429-9.

Han, X. and Xu, H. 2022. Extraction Method of Stand Density Based on High-Resolution Remote Sensing Imagery. *Journal of Physics: Conference Series* 2410 012014, doi:10.1088/1742-6596/2410/1/012014.

Hartoyo, A.P.P., Prasetyo, L.B., Siregar, I.Z., Supriyanto, Theilade, I. and Siregar, U.J. 2019. Carbon stock assessment using forest canopy density mapper in agroforestry land in Berau, East Kalimantan, Indonesia. *Biodiversitas* 20(9):2661‒2676, doi:10.13057/biodiv/d200931.

Hashim, H., Latif, A.Z. and Adnan, N.A. 2019. Urban vegetation classification with NDVI threshold value method with very high resolution (VHR) Pleiades imagery. *International Archives of the Photogrammetry, Remote Sensing and Spatial Information Sciences - ISPRS Archives* 42(4/W16):237-240, doi:10.5194/isprs-archives-XLII-4-W16-237-2019.

Hestrio, Y.F., Soleh, M., Hidayat, A., Afida, H., Gunawan, H. and Maryanto, A. 2021. Satellite data receiving antenna system for Pleiades neo observation satellite. *Journal of Physics: Conference Series* 1763:012019, doi:10.1088/1742-6596/1763/1/012019.

Huang, S., Tang, L., Hupy, J.P., Wang, Y. and Shao, G. 2021. A commentary review on the use of normalized difference vegetation index (NDVI) in the era of popular remote sensing. *Journal of Forestry Research* 32(1):1-6, doi:10.1007/s11676-020-01155-1.

Jaelani, L.M. and Putri, K. 2019. Analisis kemampuan Citra Satelit Pleiades-1B dalam mengestimasi kedalaman perairan Gili Iyang dengan menerapkan Geographically Weighted Regression (GWR). *Geoid*, *Journal of Geodesy and Geomatics* 14(2):28-34, doi:10.12962/J24423998.V14I2.3877.

Khan, K., Listyanto, T. and Soraya, E. 2022. Moisture content, density, and allometric model for estimating above-ground biomass of *Peronema canescens* trees in the private forest. *Biodiversitas* 23(2):1132-1139, doi:10.13057/BIODIV/D230258.

Kusuma, A.F., Sadono, R. and Wardhana, W. 2022. Ten years assessment of shifting cultivation on land cover and carbon storage in Timor Island, Indonesia. *Floresta e Ambient* 29 (4):e20220016, doi:10.1590/2179-8087-FLORAM-2022-0016.

Larekeng, S.H., Nursaputra, M., Nasri, N., Hamzah, A.S., Mustari, A.S., Arif, A.R., Ambodo, A.P., Lawang, Y. and Ardiansyah, A. 2022. A diversity index model based on spatial analysis to estimate high conservation value in a mining area. *Forest and Society* 6(1):142- 156, doi:10.24259/fs.v6i1.12919.

Le Maire, G., Marsden, C., Nouvellon, Y., Grinand, C., Hakamada, R., Stape, J. L. and Laclau, J.P. 2011. MODIS NDVI time-series allow the monitoring of Eucalyptus plantation biomass. *Remote Sensing of Environment* 115(10):2613-2625, doi:10.1016/j.rse.2011.05.017.

Marelign, M.A. and Mekonen, D.T. 2022. Estimating and mapping woodland biomass and carbon using Landsat 8 vegetation index: A case study in Dirmaga Watershed, Ethiopia. *Computational Ecology and Software* 12(2):67-79.

Marimpan, L.S., Purwanto, R.H., Wardhana, W. and Sumardi, 2022. Carbon storage potential of *Eucalyptus urophylla* at several density levels and forest management types in dry land ecosystems. *Biodiversitas* 23(6):2830-2837, doi:10.13057/biodiv/d230607.

Marimpan, L.S. 2023. Analysis of Carbon Stocks and Factors That Influence the Ampupu (Eucalyptus urophylla) Natural Forest in the Mutis Timau Area, East Nusa Tenggara Province. Faculty of Foretry, Univesitas Gadjah Mada. Disertation (*in Indonesian*).

Mitchell, A.L., Rosenqvist, A. and Mora, B. 2017. Current remote sensing approaches to monitoring forest degradation in support of countries measurement, reporting and verification (MRV) systems for REDD+. *Carbon Balance and Management* 12:9, doi:10.1186/s13021-017-0078-9.

Pang, Z., Zhang, G., Tan, S., Yang, Z. and Wu, X. 2022. Improving the Accuracy of Estimating Forest Carbon Density Using the Tree Species Classification Method. *Forests* 13:2004, doi:10.3390/f13122004.

Pu, R., Landry, S. and Yu, Q. 2018. Assessing the potential of multi-seasonal high resolution Pléiades satellite imagery for mapping urban tree species. *International Journal of Applied Earth Observation and Geoinformation* 71:144- 158, doi:10.1016/j.jag.2018.05.005.

Qin, H., Zhou, W., Yao, Y. and Wang, W. 2021. Estimating aboveground carbon stock at the scale of individual trees in subtropical forests using UAV LiDAR and hyperspectral data. *Remote Sensing* 13:4969, doi:10.3390/rs13244969.

Sadono, R., Pujiono, E. and Lestari, L. 2020b. Land cover changes and carbon storage before and after community forestry program in Bleberan village, Gunungkidul, Indonesia, 1999-2018. *Forest Science and Technology* 16(3):134-144, doi:10.1080/21580103.2020.1801523.

Sadono, R., Wardhana, W., Idris, F. and Wirabuana, P.Y.A.P. 2023a. Estimating carbon storage of *Eucalyptus urophylla* vegetation in Mutis Timau Nature

Reserve, East Nusa Tenggara, Indonesia using remote sensing analysis. *Biodiversitas* 24(4):1946-1952, doi:10.13057/biodiv/d240402.

Sadono, R., Wardhana, W., Idris, F. and Wirabuana, P.Y.A.P. 2023b. Developing energy production from Eucalyptus urophylla plantation in dryland ecosystem at East Nusa Tenggara, Indonesia. *Journal of Degraded and Mining Lands Management* 10(4):4673-4681, doi:10.15243/jdmlm.2023.104.4673.

Sadono, R., Wardhana, W., Wirabuana, P.Y.A.P. and Idris, F. 2020a. Productivity evaluation of *Eucalyptus urophylla* plantation established in dryland ecosystems, East Nusa Tenggara. *Journal of Degraded and Mining Lands Management* 8(1):2502-2458, doi:10.15243/jdmlm.2020.081.2461.

Samsuri, Zaitunah, A., Meliani, S., Syahputra, O.K., Budiharta, S., Susilowati, A., Rambe, R., Ulfa, M., Harahap, M.M., Arinah, H., Elfiati, D., Rangkuti, A.B., Sucipto, T., Hakim, L., Iswanto, A.H., Manurung, H. and Azhar I. 2021. Mapping of mangrove forest tree density using SENTINEL 2A satelit image in remained natural mangrove forest of Sumatra eastern coastal. *IOP Conference Series: Earth and Environmental Science* 912 012001, doi:10.1088/1755-1315/912/1/012001.

Shah, S. and Sharma, D.P. 2023. Monitoring carbon stock changes in Solan Forest Division of Indian Western Himalayas. *Environment, Development and Sustainability*, doi:10.1007/s10668-023-03040-3.

Sousa, A.M., Gonçalves, A.C., Mesquita, P. and da Silva, J.R.M. 2015. Biomass estimation with high resolution satellite images: A case study of Quercus rotundifolia. *ISPRS Journal of Photogrammetry and Remote Sensing* 101:69-79, doi:10.1016/j.isprsjprs.2014.12.004.

Sukarna, R.M., Birawa, C. and Junaedi, A. 2021. Mapping above-ground carbon stock of secondary peat swamp forest using forest canopy density model Landsat 8 OLI-TIRS: A case study in Central Kalimantan Indonesia. *Environment and Natural Resources Journal* 19(2):165-175, doi:10.32526/ennrj/19/2020209.

Tian, L., Wu, X., Tao, Y., Li, M., Qian, C., Liao, L. and Fu, W. 2023. Review of remote sensing-based methods for forest aboveground biomass estimation: progress, challenges, and prospects. *Forests* 14(6):1-31, doi:10.3390/f14061086.

Tosiani, A. 2015. Carbon Absorption and Emission Activity Book. Directorate of Forest Resources Inventory and Monitoring Directorate General of Forestry Planning and Environmental Management Ministry of the Environment. Jakarta (*in Indonesian*).

Trigozo, J.P.R., Oré Cierto, L.E., Aliaga, W.C.L. and Oré Cierto, J.D. 2021. Carbon stored in forest plantations in The Mariano Dámaso Beraún District, Huánuco – Perú. *Revista Científica Yotantsipanko* 1(1):32-43, doi:10.54288/YOTANTSIPANKO.V1I1.6.

Vega-Puga, M., Romo-Leon, J.R., Castellanos, A.E., Castillo-Gámez, R.A., Garatuza-Payán, J. and Ángeles-Pérez, G. 2023. High resolution images for change detection on aboveground carbon storage in semiarid communities, after the introduction of exotic species *Cenchrus ciliaris*. *Botanical Sciences* [S.l.] 101(1):41-56, doi:10.17129/botsci.3026.

Viana, H., Aranha, J., Lopes, D. and Cohen, W.B. 2012. Estimation of crown biomass of *Pinus pinaster* stands and shrubland above-ground biomass using forest inventory data, remotely sensed imagery and spatial prediction models. *Ecological Modelling* 226:22-35, doi:10.1016/j.ecolmodel.2011.11.027.

Wang, D., Wan, B., Qiu, P., Su, Y., Guo, Q., Wang, R., Sun, F. and Wu, X. 2018. Evaluating the performance of Sentinel-2, Landsat 8 and Pléiades-1 in mapping mangrove extent and species. *Remote Sensing* 10:1468, doi:10.3390/rs10091468.

Wang, S., Zhang, X., Hassan, M.A., Chen, Q., Li, C., Tang, Z. and Wang, Y. 2018. QuickBird image-based estimation of tree stand density using local maxima filtering method: A case study in a Beijing forest. *PLoS ONE* 13(12):e0208256, doi:10.1371/journal.pone.0208256.

Zhang, F., Tian, X., Zhang, H. and Jiang, M. 2022. Estimation of aboveground carbon density of forests using deep learning and multisource remote sensing. *Remote Sensing* 14(13):3022, doi:10.3390/rs14133022.